Solid State Science and Technology, Vol. 27, No 1 & 2 (2019) 105-121
ISSN 0128-7389 | *http://myjms.moe.gov.my/index.php/masshp*

T1 AND T2 CHARACTERISTICS OF POLY(VINYL) ALCOHOL SLIME PHANTOM WITH DIFFERENT RELAXATION MODIFIER CONCENTRATIONS

Yee Ying Yih[1], Tee Hui Sin[1], Nurul Ain Ayuni Azhar[1], Hanani Abdul Manan[2], Mohd Nor Affendi Awang[3] and *Ahmad Nazlim Yusoff[1]

[1]*Diagnostic Imaging and Radiotherapy Program, Centre for Applied Health Sciences, Faculty of Health Sciences, Universiti Kebangsaan Malaysia, Jalan Raja Muda Abdul Aziz, 50300 Kuala Lumpur, Malaysia*

[2]*Deparment of Radiology, Faculty of Medicine, Universiti Kebangsaan Malaysia Medical Centre, Jalan Yaakob Latiff, 56000 Bandar Tun Razak, Cheras, Kuala Lumpur, Malaysia*

[3]*Department of Radiology, Hospital Canselor Tuanku Muhriz, Universiti Kebangsaan Malaysia Medical Centre, Jalan Yaakob Latiff, 56000 Bandar Tun Razak, Cheras, Kuala Lumpur, Malaysia*

**Corresponding author:* nazlimtrw@ukm.edu.my

ABSTRACT

Many studies have been carried out to produce magnetic resonance imaging (MRI) phantom which is inexpensive, non-hazardous, easy to produce, mimic human tissue and has good SNR homogeneity. Among those that were studied were poly(vinyl) alcohol (PVA) slime phantoms. The characteristics of PVA slime phantom chosen for this study include naturally flexible, tough and has relaxation times close to human tissue. The objectives of this study were to investigate the T1 and T2 characteristics of the PVA slime phantom with different relaxation modifier (gadolinium (III) oxide, Gd_2O_3) concentrations and to determine its suitability as alternative to agarose gel phantom. Five PVA slime phantoms were prepared by mixing PVA and borax solution at a fixed ratio but with the addition of different quantity of Gd_2O_3. The T1 (fixed echo time (TE) and different repetition time (TR)) and T2 (fixed TR and different TE) weighted images of all phantoms including distilled water were acquired using SIEMENS Magnetom Verio 3-tesla MRI system at the Radiology Department, Hospital Canselor Tuanku Muhriz (HCTM) via spin echo (SE) and turbo spin echo (TSE) sequences respectively. The signal-to-noise ratio (SNR) of all phantoms was calculated using Image-J software (The National Institutes of Health, NIH) by implementing the region of interest (ROI) analysis. The SNR vs TR and SNR vs TE curves were fitted to the exponential equations for T1 and T2 relaxation using MATLAB® R2018b (The Math Works, Inc., Natick) to determine the T1, T2 and saturation (SNR_o). For all phantoms, T1 curves demonstrated that the SNR increases exponentially with increasing TR (constant TE) while T2 curves showed that the SNR decreases exponentially with increasing TE (constant TR). Gd was found to affect the T1 but not

the T2 curves. SNR_0, T1 and T2 relaxation times decrease with increasing Gd_2O_3 concentration. It can be concluded that with a systematic increase in the quantity of relaxation modifier, the T1 and T2 relaxation times decrease in a systematic manner. Further studies are necessary to investigate the stability of the PVA slime phantom over a long period of time.

Keywords: Poly(vinyl) alcohol, sodium tetraborate; gadolinium oxide; TR; longitudinal magnetization; TE; transverse magnetization

INTRODUCTION

Magnetic resonance imaging (MRI), formerly known as nuclear magnetic resonance (NMR) operates based on the interaction between the nucleus spin and magnetic field. It works around the change in the longitudinal and transversal magnetizations of tissues. Due to its high spatial and temporal resolutions and unique ability to distinguish between different types of soft tissues without using ionizing radiation, its demand in the medical field increases each year. With MRI scanners being extensively used in clinical and research settings, they are prone to technical and image quality problems. Thus, quality control (QC) is important and necessary in order to maintain good diagnostic quality of MRI images produced [1].

MRI phantom is an important apparatus in QC of MRI. The development of a multipurpose phantom is advantageous in MRI QC especially in the testing of instrument performances and evaluating new imaging techniques and sequences. The multipurpose phantom would also allow system comparisons to be made [2]. It is also very useful in the development of new pulse sequences, adjustment of operational conditions, technical training of operators, delineating specific organs and evaluation of safety [3 & 4]. A good MRI phantom should have relaxation times and dielectric properties equivalent to human tissues, homogenous relaxation times and dielectric properties throughout the phantom, sufficient strength to fabricate a torso without the use of physical reinforcements, allowing fabrication in the shape of human organs, the ease of handling and chemical and physical stability over an extended period of time [5]. Furthermore, the materials used for MRI phantom should be toxic-free as the phantom might be broken during shipping and would lead to contamination of MRI instrument, staff and researchers [6].

Over the decades, many materials that mimic human tissues have been studied and proposed [7 – 9]. The materials should fulfil characteristics such as inexpensive, non-toxic, easy to handle, easily prepared, stable over a long period of time and should possess properties of tissues. Thus it is essential to determine the most ideal material for the MRI phantom. Agarose gel has been commonly used as phantom materials in previous studies [3 – 9]. The main concern of using agarose gel as phantom material is that it is produced naturally, which can be considered as an advantage but its relaxation properties differ between different batches of production [3]. Additionally, in terms of long-term stability, agarose gel phantom tends to deteriorate over time. Water loss from

the gel phantom will cause the breakdown of the phantom at the same time causing a change in the relaxation times [9, 10]. On the other hand, synthetic polymers such as PVA are standardized thus they do not differ in the relaxation properties [3]. Therefore, this study is carried out to explore the potential of other materials such as poly(vinyl) alcohol (PVA) slime as MRI phantom.

PVA is a non-toxic, hydrophilic, synthetic polymer recently introduced in tissue engineering for biocompatibility [11]. It is generally safe to be used as MRI phantom materials. Previous study [12] found that PVA gel can be used to construct MRI phantom because of its suitable characteristics and properties including compatibility with other substances, homogenous, shape retaining capability and having values of T1 and T2 similar to human soft tissues. In another study [13] using PVA cryogel as MRI phantom material, a near ideal material for distensible phantoms was successfully fabricated. Its homogenous signal intensity, relaxation times close to human tissue and inherently flexible and tough made it a near ideal phantom material. Although studies have shown that PVA gel was a good substitute for MRI phantom material, its long-term stability remains unknown.

Borax, also known as sodium tetraborate with a chemical formula of [$Na_2B_4O_7 \cdot 10H_2O$] is a strong alkaline that can be hydrolyze in water to produce boric acid-borate buffer having approximately a pH of 9 [14]. It works together with PVA glue to form slime which will be used as the phantom materials for this study. One of the most common way to produce slime is by adding saturated solution of sodium tetraborate (borax) to a solution of white glue and water. As a result of the crosslinking between the protein molecules of the white glue and the borate ions ($B(OH)_4^-$) of the borax solution, a highly viscos slime is formed. Alternatively, an aqueous PVA can be used in replacement of white glue.

In many cases, the magnetic properties of the phantom can be adjusted by using various additives such as graphite and paramagnetic ions [5]. The T1 and T2 relaxation times and conductivity of the phantom can be independently changed by modifying the concentration of the paramagnetic ions and the concentration of the gelling agent. Paramagnetic ions such as $CuSO_4$, $NiCl_2$, $MnCl_2$ or $GdCl_3$ have been commonly used as T1 modifiers. In this study Gd_2O_3 was used as the relaxation modifier. Gadolinium based chelates and iron oxide nanoparticles are often used as MRI contrast agent. They act as positive contrast agents because they will reduce the T1 relaxation time which leads to the increase in signal intensity when measured using the same repetition time (TR). Therefore, by modifying the concentration of paramagnetic ions such as $GdCl_3$, relaxation time and conductivity of the phantom can be altered which in turn allow the development of phantoms with a wide range of relaxation time to resemble different human tissues and organs. This is further supported by studies done by [8, 10] where the T1 value decreases with the increases of $GdCl_3$ concentration.

The objectives of this study were to determine the T1 and T2 characteristics of the PVA slime phantom with different relaxation modifier concentration and to determine the

possibility of PVA slime phantom to be used as an alternative to agarose gel phantom. The purpose of having different relaxation modifier concentration in this study was to investigate the characteristics of the optimum Gd concentration. By comparing and analysing the T1 and T2 values of the water phantom and the PVA slime phantom with different relaxation modifier concentrations, we can determine how close the characteristics of the PVA slime phantom are to human tissues. On top of that, adding relaxation modifier to the PVA slime phantom will alter the T1 and T2 relaxation times thus promoting the development of experimentally well-characterized tissues equivalent MRI phantom. It is hypothesized that with a systematic increase in the quantity of the relaxation modifier, the T1 and T2 relaxation times will decrease in a systematic manner.

EXPERIMENTAL

Chemicals and Apparatus

The chemicals used in this study are as follows: poly (vinyl) alcohol, (C4H6O2)n (Chemiz (M) Sdn. Bhd), sodium tetraborate [Na2B4O7·10H2O] (Chemiz (M) Sdn. Bhd), gadolinium (III) xide, Gd_2O_3 (HmbG® Chemicals), hydrochloric acid, HCl 37% (Fisher Scientific (M) Sdn. Bhd). The apparati used in this study include digital weighing scale (OHAUS® Pioneer PA 210C), magnetic stirrer with hotplate, steriled plastic container, beaker and 5-ml pipette. The MRI system used was a 3-T Siemens Magnetom Verio.

Preparation of PVA slime phantom

Five PVA slime phantoms with different Gd_2O_3 concentration (0 $mgml^{-1}$, 0.016 $mgml^{-1}$, 0.049 $mgml^{-1}$, 0.085 $mgml^{-1}$, 0.124 $mgml^{-1}$) were prepared. Different masses of Gd_2O_3 powder (m = 1, 3, 5 and 7 mg) were firstly weighed using the electronic weighing scale and were separately placed into four different beakers. Due to Gd_2O_3 insolubility in water, HCl acid (5 ml) was added into the four beakers. The beakers were gently stirred and set aside for approximately 15 minutes for the Gd_2O_3 powder to completely dissolve.

At the same time, 0.04% of PVA and borax solution were prepared. 16 g PVA powder was weighed using the electronic weighing scale and was slowly added to 400 ml distilled water at a temperature of 80 °C – 90 °C. The solution was stirred using magnetic stirrer with hot plate for about an hour. The appearance of the solution changed from murky to crystal clear indicates that the PVA powder is completely dissolved and the solution is in a uniform distribution state. The PVA solution was then left to cool down to room temperature. An amount of 1.6 g borax powder was weighed using the electronic weighing scale and was added to 40 ml of distilled water. The solution was stirred gently using glass rod until the borax powder was completely dissolved. The PVA, borax and Gd_2O_3 solutions were mixed together in a sterile plastic container using 50- and 20-ml syringe simultaneously. The slime was formed when the borax solution has completely reacted with the PVA solution. The container lid was air-tight closed. All the prepared phantoms were stored at room temperature in a desiccator for two days due to the busy schedule of MRI machine in the hospital. The details about

the quantity of the ingredients used were given in Table 1.

Table 1: PVA slime phantom mass and volume measurements

Sample	Volume of PVA solution/ml	Concentration of PVA/gml^{-1}	Volume of Borax solution/ml	Concentration of Borax/gml^{-1}	Mass of Gd_2O_3/mg	Concentration of Gd_2O_3/ mgml^{-1}
1	70	0.04	7	0.04	0	0
2	65	0.04	6.5	0.04	1	0.016
3	65	0.04	6.5	0.04	3	0.049
4	65	0.04	6.5	0.04	5	0.085
5	65	0.04	6.5	0.04	7	0.124

Data Acquisition and Analyses

The MRI data were acquired using Siemens Magnetom Verio 3-Tesla MRI system at the Department of Radiology, Hospital Canselor Tuanku Muhriz. The plastic container containing PVA slime phantoms and distilled water were inspected for leakage and any presence of air bubbles and foreign particles before being scanned. Examples of the prepared phantoms are shown in Figure 1(a). They were then positioned horizontally in the 32-channel head coil by using a home-made sample holder (Figure 1(b)) at the iso-centre of the magnet bore. All the six phantoms were scanned simultaneously. The spin echo (SE) and turbo spin echo (TSE) sequences were applied to obtain the axial T1 and T2 weighted images respectively. T1 weighted images were obtained using a constant TE = 15 ms and TR = 100, 150, 200, 300, 600, 800, 1000, 1200, 1800, 2400, 3600, 4800, 5600, 6400 and 8000 ms. The T2 weighted images were obtained using a constant TR = 4970 ms and TE = 69, 82, 96, 110, 123, 137, 151, 165, 178, 192, 206, 220, 233, 247 and 261 ms. Other imaging parameters include slice thickness = 3.0 mm, matrix size = 64 × 64, field of view (FOV) = 230 × 230 mm and voxel size = 0.6 ×0.4 × 3.0 mm. All the images acquired were stored in a CD-ROM in DICOM format.

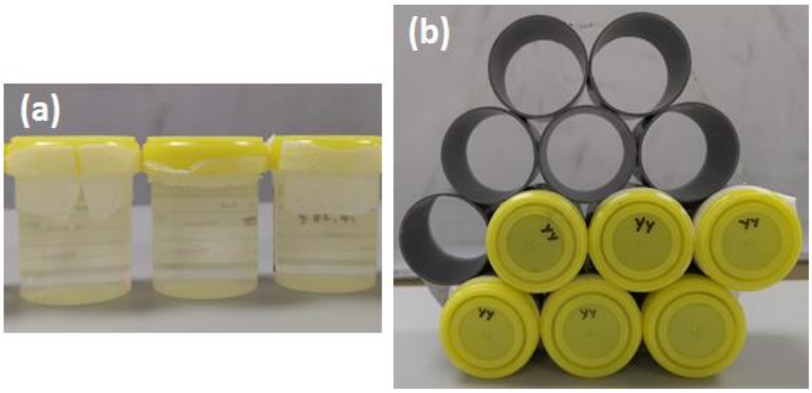

Figure 1: shows the example of phantoms prepared in the plastic container (a) and the orientation of the phantoms inside the sample holder (b)

Image-J software (The National Institutes of Health, NIH) was used to measure the signal-to-noise ratio (SNR) for all phantoms. The middle slice from each volume measurement of the phantoms was chosen for SNR evaluation. The image selected was visually ensured to have a spatially homogenous distribution of signal intensity [15]. From the acquired images, the mean signal intensity of the phantom (I_p), signal intensity of the background noise (I_b) and standard deviation of the background noise (σ_b) were computed. Three circularly shaped ROIs with the size of 5 mm^2 were specified on the phantom images and I_p were obtained and averaged. Another circularly shaped ROI with the size of 40 cm^2 was drawn at the background, outside of the phantom images in order to obtain I_b and σ_b. The SNR value for each phantom across all TEs and TRs were then calculated using the formula $SNR = (I_p - I_b)/\sigma_b$.

T1, T2, SNR_o, 1/T1 and 1/T2 Determination

The T1 and T2 values of the phantoms were determined based on the SNR vs TR plot (T1 curve) with the equation of $SNR \propto 1 - e^{-TR/T1}$ and SNR vs TE plot (T2 curve) with the equation of $SNR \propto e^{-TE/T2}$ respectively. The experimental data were fitted to both the equations using MATLAB® R2018b (The Math Works, Inc., Natick) curve fitting toolbox. The T1 and T2 values were obtained upon achieving the minimum sum of squared difference between the observed and fitted data. Likewise, by referring to the fitted T1 curve, the saturation value (SNR_o) was also determined. The 95% confidence interval (CI), standard sum of errors (SSE) and the R^2 of fit were also computed. The R-square of fit is the correlation coefficient between the observed and fitted data and the ideal value of R-square is 1. The T1 and T2 curves in this study were fitted in such way that the R^2 of fit is maximized and the SSE is minimized.

Consequently, the inverse of T1 and T2 relaxation times were calculated and curve fitted using the same toolbox to obtain the relaxation rates, r_1 (1/T1) and r_2 (1/T2). The effects of different Gd_2O_3 concentration on T1, T2, SNR_o, r_1 and r_2 were evaluated and studied.

RESULTS

Figure 2 (a) and (b) are the examples of spin echo T1 weighted images at TR = 1800 ms, TE = 15 ms and turbo spin echo T2 weighted images at TE = 123 ms, TR = 4970 ms for all six phantoms. A is the image of distilled water, B is the image of pure PVA slime phantom without addition of Gd_2O_3, C is the image of PVA slime phantom with 0.016 $mgml^{-1}$ of Gd_2O_3, D is the image of PVA slime phantom with 0.049 $mgml^{-1}$ Gd_2O_3, E is the image of PVA slime phantom with 0.085 $mgml^{-1}$ Gd_2O_3 and finally F is the image of PVA slime phantom with 0.124 $mgml^{-1}$ Gd_2O_3. The SNR obtained from the acquired T1 and T2 weighted images are summarized in Tables 2 and 3 respectively.

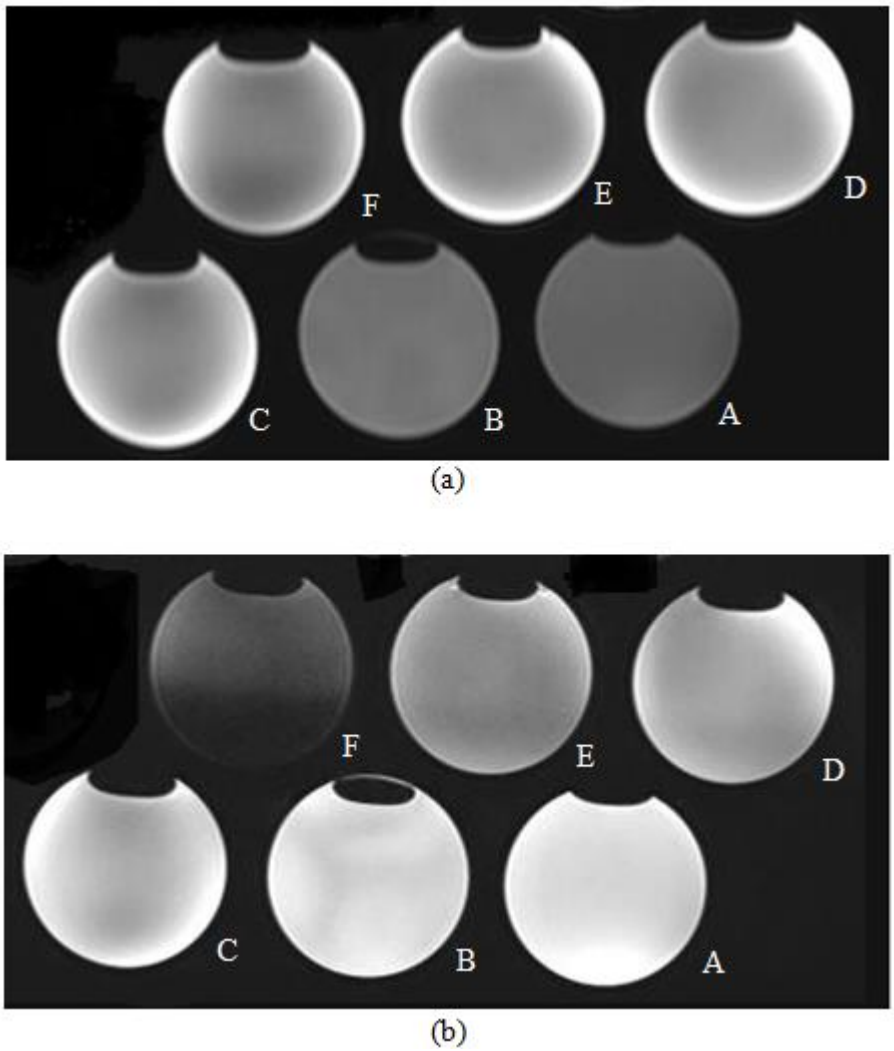

Figure 2: (a) T1 weighted images for all phantoms, TR = 1800 ms, TE = 15 ms; (b) T2 weighted images for all phantoms, TE = 123 ms, TR = 4970 ms. Images A – F belong to different phantoms as mentioned in the text

It can be seen from Figure 2 that the intensity of all images and background is homogenous. For both distilled water (A) and pure PVA slime phantom (B) the intensity of the T2 weighted images is higher than the T1 weighted images. For T1 weighted images, the signal intensity of the phantoms decreases with the addition of Gd_2O_3. Similarly, for the T2 weighted images, the signal intensity decreases with the addition of Gd_2O_3. It was also found that the intensity of the images obtained from each particular sample changes for different combination of TR and TE values. Those images are not shown but the corresponding SNR data are given in the following tables.

Table 2: The SNR value of all phantoms at fixed TE value (15 ms) and different TR values between 100 and 8000 ms. The T1 relaxation time of each phantom with different concentration of relaxation modifier is obtained from the curve fitting method

Phantoms	TR/ms														
	100	150	200	300	600	800	1000	1200	1800	2400	3600	4800	5600	6400	8000
Water	6.88	12.24	17.33	27.64	59.38	80.82	97.75	114.52	171.03	207.75	273.34	336.16	358.47	376.46	446.77
1	10.43	17.18	24.72	38.07	78.02	105.99	125.69	145.10	212.25	252.85	324.10	390.90	411.16	427.53	496.37
2	41.46	60.66	77.71	108.20	179.24	212.86	220.68	229.90	259.77	255.85	259.04	274.59	277.94	284.63	316.53
3	44.71	77.61	99.04	135.14	207.42	239.99	252.83	258.01	272.53	264.29	267.63	277.13	271.63	269.88	295.38
4	63.21	98.16	121.19	156.89	220.20	242.79	242.51	242.29	254.27	244.92	241.68	250.22	247.49	245.44	266.15
5	113.54	155.28	173.66	191.55	218.14	227.93	228.65	227.18	237.52	229.67	227.23	235.60	232.63	230.62	250.09

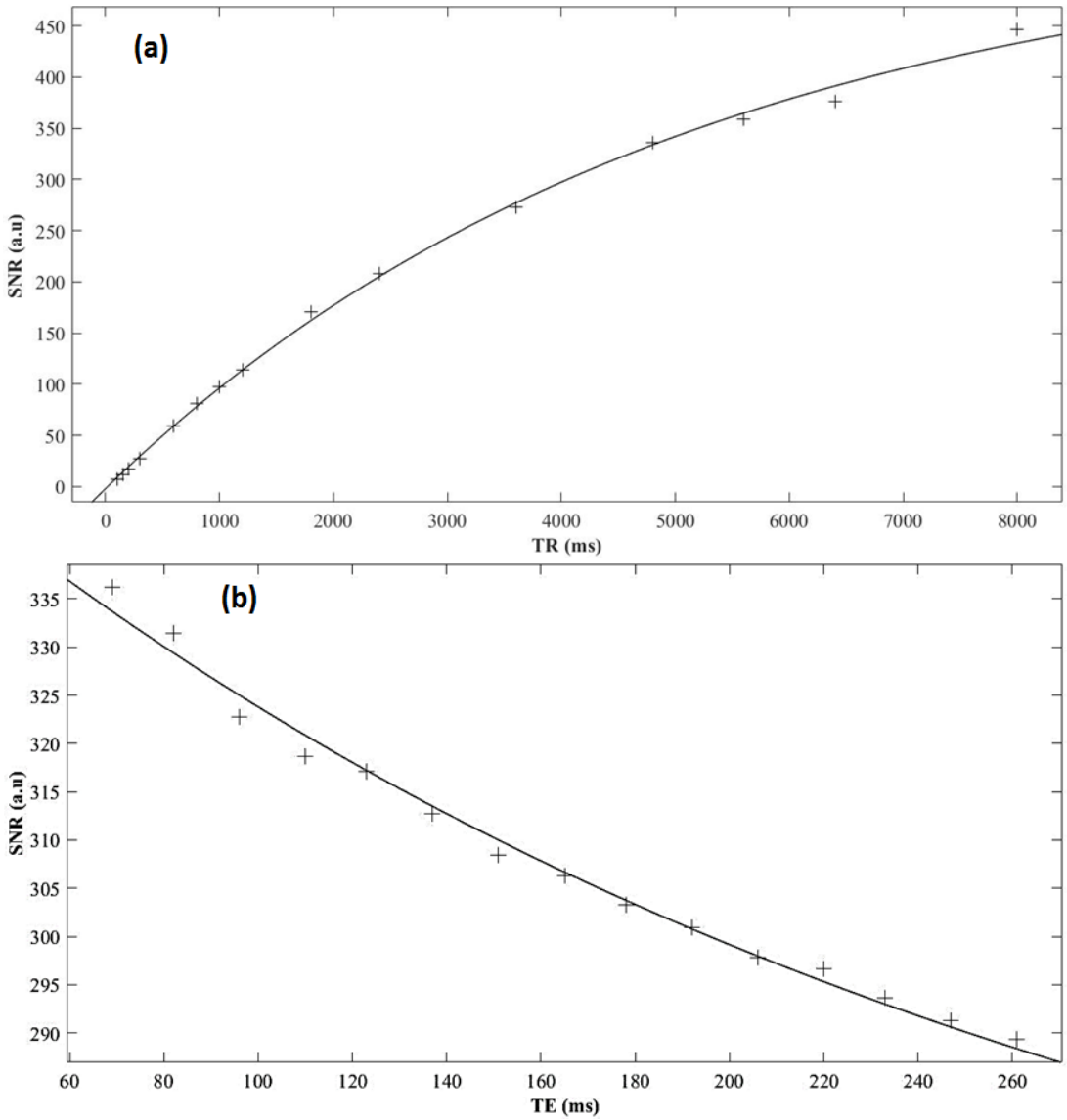

Figure 3 (a) SNR vs TR, TE = 15ms; (b) SNR vs TE, TR = 4970ms curves for distilled water phantom

Distilled water phantom

Figure 3 (a) and (b) show the results obtained from the measurement of SNR as a function of TR and TE respectively for the distilled water phantom. The exponential model was fitted to the experimental data using MATLAB® R2018b (The Math Works, Inc., Natick) curve fitting toolbox to obtain the fitted T1 and T2 curves. The symbol + represents the experimental data while the line is the fitted curve. It can be clearly observed that the data obtained fulfilled the exponential behaviour of the form $SNR \propto 1 - e^{-TR/T1}$ for T1 curve and of $SNR \propto e^{-TE/T2}$ for T2 curve. By using non-linear least square fitting method, the T1 and T2 relaxation times of the distilled water phantom obtained was 5051 ms and 246 ms respectively. When compared to the T1 and T2 values of standard MRI water phantom which are 2612 ms and 212 ms respectively, the distilled water phantom has longer T1 and T2 relaxation times and the difference is larger for T1. This might be due to the presence of $NiSO_4$ in the standard MRI water phantom that acts as relaxation modifier and increased the T1 relaxation rate (1/T1) significantly.

The results obtained from the distilled water phantom therefore verify the exponential increase of T1 with increasing TR and exponential decrease of T2 with increasing TE. The T1 of the distilled water obtained from this study is about 20 times longer than T2. This further validates the methods used for this study on PVA slime phantom.

Effect of Gd_2O_3 on the relaxation, saturation and relaxation rate of PVA Slime Phantom

The SNR values for all phantoms at fixed TE (15 ms) and different TR are tabulated in Table 2 while the SNR values for all phantoms at fixed TR (4970 ms) and different TE are tabulated in Table 3. Figure 4 (a) and (b) are the T1 and T2 relaxation curves for different Gd_2O_3 concentrations plotted using the SNR data shown in Table 2 and 3.

Table 3 The SNR value of all phantoms at fixed TR value (4970 ms) and different TE value between 69 and 261 ms. The T2 relaxation time of each phantom with different concentration of relaxation modifier is obtained from the curve fitting method

Phantoms	TE/ms														
	69	82	96	110	123	137	151	165	178	192	206	220	233	247	261
Distilled water	336.25	331.39	322.73	318.71	317.14	312.69	308.46	306.32	303.32	300.90	297.80	296.60	293.60	291.28	289.30
1	234.41	233.53	206.87	205.15	200.72	196.37	189.92	185.46	174.01	171.19	167.83	160.71	159.42	153.69	151.71
2	172.89	169.09	167.27	164.36	154.77	149.19	144.99	138.13	134.20	132.88	127.99	123.19	120.62	114.26	112.37
3	179.38	167.30	154.17	155.78	142.67	134.59	128.14	116.71	113.63	109.42	101.90	96.41	93.01	85.10	84.78
4	157.02	140.24	130.21	128.56	114.27	105.29	98.92	86.66	83.68	78.15	71.57	65.56	61.89	57.24	53.98
5	99.04	84.45	74.58	65.11	53.11	46.80	42.04	34.26	30.13	25.55	21.38	17.38	15.37	14.68	10.57

Table 4: (a) T1 values, 95% confidence interval (CI), standard sum of error (SSE), R-square of fit (correlation coefficient between observed and fitted data), saturation (SNR_o), and relaxation rate for all phantoms, (b) similar data for T2

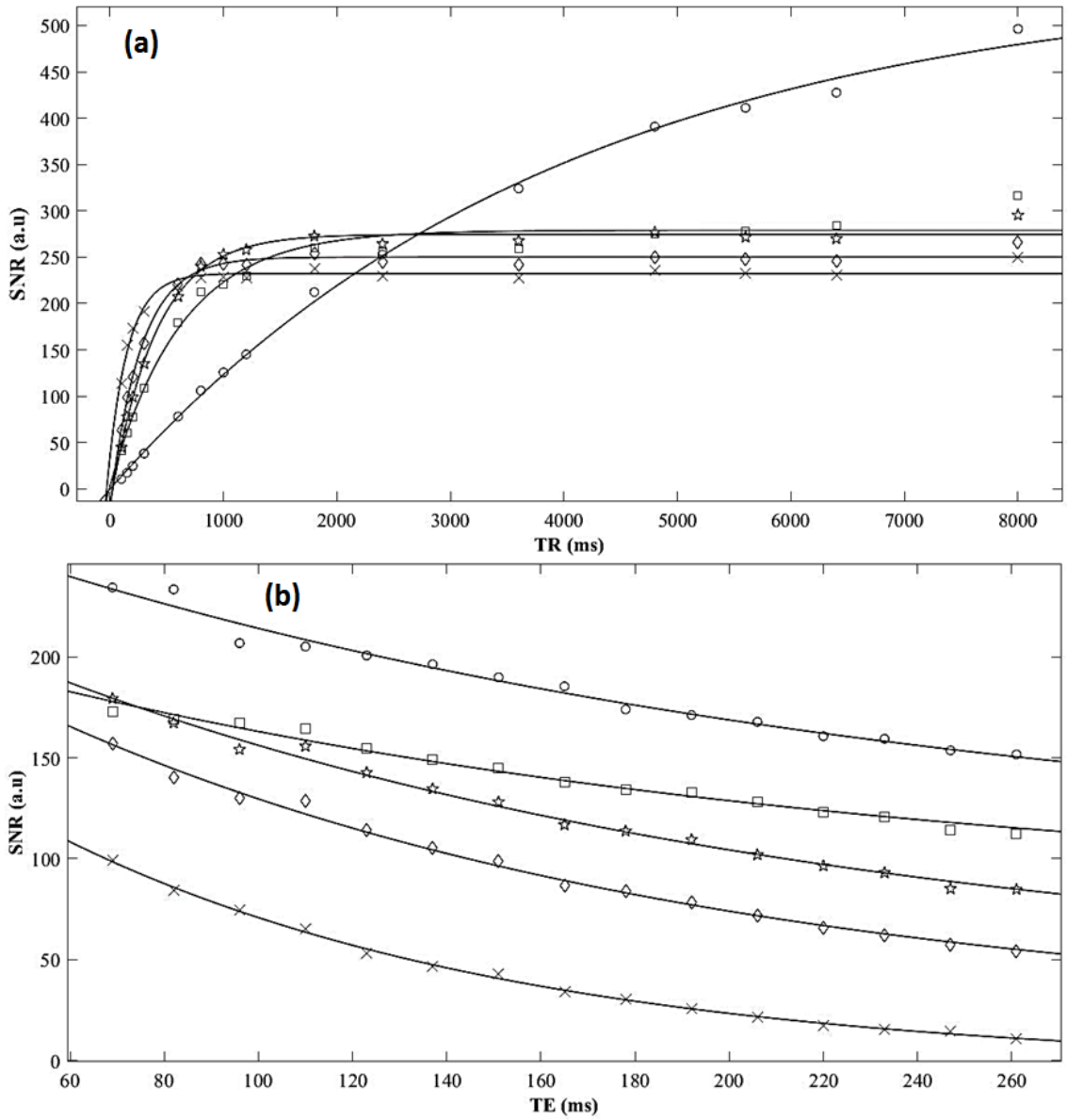

Figure 4: (a) SNR vs TR, TE = 15 ms; (b) SNR vs TE, TR = 4970 ms curves for all phantoms containing different Gd_2O_3 concentrations; 0 $mgml^{-1}$ (○), 0.016 $mgml^{-1}$ (□), 0.049 $mgml^{-1}$ (☆), 0.0085$mgml^{-1}$ (◇) and 0.124 $mgml^{-1}$ (×). Solid lines are the fitted curves

(a)

T1 curve fitting parameters

Sample	T1/ms	95% CI for T1/ms	SSE for T1	R-square of fit	SNR_o	r_1/s^{-1}
Distilled water	5051.0	4242.0, 5861.0	574.7	0.998	547.2	0.198
1	3948.0	3395.0, 4496.0	790.8	0.998	552.8	0.253
2	626.9	474.8, 778.9	2371.0	0.979	276.1	1.595
3	476.6	414.8, 53.3	1358.0	0.986	262.0	2.098
4	328.7	290.0, 366.5	832.6	0.986	236.6	3.042
5	177.5	118.5, 236.6	631.1	0.968	197.1	5.634

(b)

T2 curve fitting parameters

Sample	T2/ms	95% CI for T2/ms	SSE for T2	R-square of fit	r_2/s^{-1}
Distilled water	246.0	231.4, 260.6	26.9	0.991	4.065
1	197.3	179.1, 215.5	209.4	0.979	5.068
2	187.7	171.6, 203.7	101.9	0.983	5.328
3	169.2	159.7, 178.7	97.5	0.992	5.910
4	141.2	133.9, 148.4	88.6	0.994	7.082
5	97.5	86.7, 108.3	19.6	0.998	10.257

The T1 curve for the pure PVA slime phantom increases exponentially as TR increases when TE was fixed at 15 ms. The curve is obviously different when compared with the curves for PVA slime phantom containing Gd_2O_3 from which it can be seen that the increase in SNR is gradual when TR increases with no sign of saturation in the range of TR used. For the Gd_2O_3-containing phantoms, the increase in SNR is rapid with a sign of decreasing T1 relaxation time with increasing Gd_2O_3 concentration for TR < 1000 ms and the curves indicate saturation when TR > 1000 ms. Furthermore, pure PVA slime phantom shows the highest SNRo but for the Gd_2O_3 containing phantoms, SNRo seems to decrease with increasing Gd_2O_3 concentration. In Figure 4(b), an exponential decrease in SNR can be observed for all phantoms when TE is increased (TR fixed at

4970 ms). The pattern looks similar for all phantoms with a sign of constant T2 relaxation time. It is however obvious that the SNR at any TE values decreases with increasing Gd_2O_3 concentration. The results indicate a larger influence of Gd_2O_3 concentration on T1 relaxation as compared to its influence on T2 relaxation.

The T1 and T2 values for all phantoms obtain from curve fitting method are shown in Table 4 together with the curve fitting statistics. T1 was found to decreases from 3948 ms to 177.5 ms with the increase in Gd_2O_3 concentration from 0 $mgml^{-1}$ to 0.124 $mgml^{-1}$ while T2 decreases from 197.3 ms to 97.49 ms with the increase in Gd_2O_3 concentration from 0 $mgml^{-1}$ to 0.124 $mgml^{-1}$. The decrease in T1 is larger than the decrease in T2 with the increase in Gd_2O_3 concentration. The results indicate a larger effect of Gd_2O_3 concentration on T1 as compared to its effect on T2.

The saturation (SNR_o) values for all phantoms obtained from curve fitting method are tabulated in Table 4. The SNR_o for distilled water is also provided for comparison. The SNR_o values decreases from 552.8 to 197.1 with the increase in Gd_2O_3 concentration from 0 $mgml^{-1}$ to 0.124 $mgml^{-1}$. The SNR_o values for the phantoms demonstrate a similar trend as the T1 values from which the SNR_o decreases gradually with the increase of Gd_2O_3 concentration. The change can be visualized in Figure 5. Note an initial rapid drop in the T1 and SNR_o as the Gd_2O_3 is gradually increased.

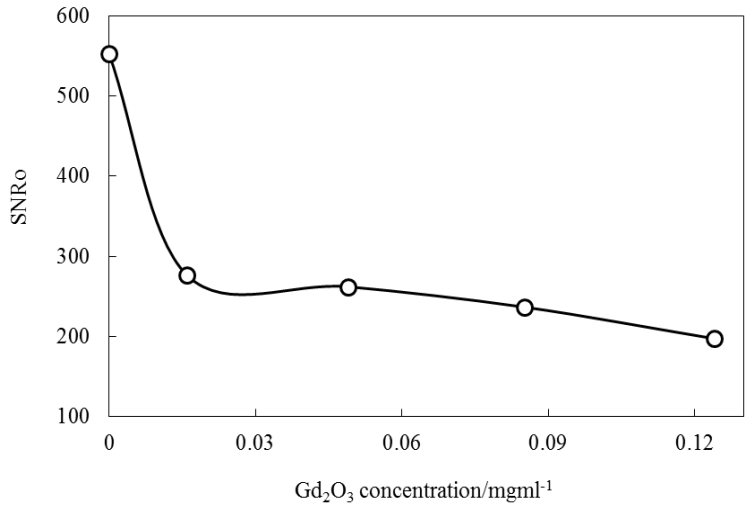

Figure 5: Saturation (SNRo) vs different Gd_2O_3 concentration obtained from T1 curve

The change in r_1 and r_2 of the PVA slime phantom as a function of Gd_2O_3 concentration are shown in Figure 6 together with the fitted line. The individual data can be found in Table 4. Both the r_1 and r_2 show a linear relationship with Gd_2O_3 concentration with r_2 higher than r_1 for all Gd_2O_3 concentrations. The gradient of the slopes as determined from the fitted line are 38.5 $mM^{-1}s^{-1}$ and 39.5 $mM^{-1}s^{-1}$ for r_1 and r_2 respectively.

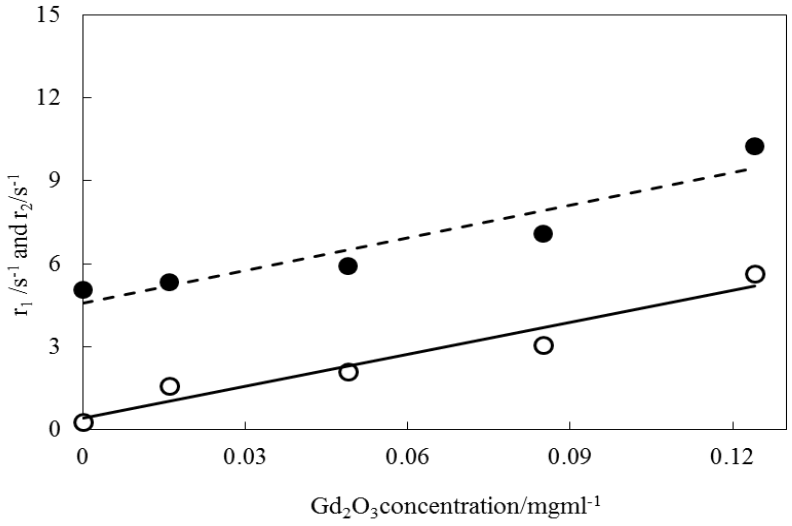

Figure 6 Inverse of relaxation times (O: 1/T1 = r_1 and ●: 1/T2 = r_2) (also known as relaxation rate: how fast magnetisation/SNR change in one second) vs. different Gd_2O_3 concentration

DISCUSSION

The PVA slime phantom used in this study demonstrated similar relaxation properties as shown by distilled water phantom hence human tissue because human tissue contains a lot of water. The exponential increase of SNR value as a function of TR for distilled water phantom and PVA slime phantom is the manifestation of the gradual increase of longitudinal magnetization with time. This typical T1 relaxation phenomenon resemble spin-lattice energy transfer in which the net magnetization in z direction returns to its initial maximum value parallel to the magnetic field after being resonated into the transverse plane by a 90° radiofrequency (RF) pulse. The magnetization behaviour is represented by the T1 curve. If TR is sufficiently long, the magnetization in the z direction has more time to regain its magnitude and reaches the saturation (indicated as SNR_o) which can be clearly seen for all phantoms that contain Gd_2O_3 (Figure 4(a)). The SNR_o for these phantoms can be determined precisely from the plots but for the sake of precision, they were also obtained from the fitting method implemented in this study. The distilled water phantom and pure PVA slime phantom showed a higher SNR_o value (547.2 and 552.8 respectively) as compared to Gd_2O_3 – contained PVA slime phantom as they contain a higher density of hydrogen protons. For the Gd_2O_3 contained phantoms, the SNRo is lower despite the existence of magnetic element (Gd) in the lattice.

The addition of Gd_2O_3 into the lattice has two main effects on the T1 curves. First, it decreases the saturation of the curve and second it shortened the relaxation of the spins and shifted the curve to the left for TR values less than 1000 ms. Gd_2O_3 is chemically

stable with two Gd^{3+} ions being attached to three O^{2-} ions. At room temperature, Gd_2O_3 formed a cubic structure, electrostatically neutral but possesses magnetic susceptibility of about 53.2×10^{-6} cm^3/mol. For the first effect, by increasing the number of Gd_2O_3 molecules in the PVA slime phantoms while keeping the weight of the phantom constant, the number of water molecules was reduced. This will cause a reduction in the SNR_o because SNR_o is largely influenced by the density of water in the PVA slime phantom. For the pure PVA slime phantom, the SNRo is highest because the water molecules were not replaced with the Gd_2O_3 molecules. For the Gd_2O_3 added PVA slime phantoms, the SNR_o decreases systematically with increasing Gd_2O_3 concentration, see Figure 5. A marked drop in SNR_o from pure PVA slime phantom to the first Gd_2O_3 added phantom, followed by a small change in SNR_o for the subsequent addition of Gd_2O_3 indicates that the addition of Gd_2O_3 only has a significant effect on SNR_o only when a small quantity of Gd_2O_3 is used. Further increase in Gd_2O_3 will only cause a small change in the SNR_o.

For the second effect, the theory of magnetic dipole-dipole interaction can be used to explain the change in the T1 relaxation of the PVA slime phantoms. Dipole-dipole interaction is the most important mechanism for magnetic relaxation in biological tissues. Spins (or spin angular momentums) in the distilled water, pure PVA and Gd_2O_3 – contained PVA slime phantoms can be thought of as tiny magnets with north and south poles, each of which produces magnetic fields. As the spins precess, their magnetic fields interact with one another and with the magnetic fields of the lattice causing changes magnetic field inhomogeneity. Without the presence of Gd_2O_3, the T1 relaxation takes longer time as shown by distilled water and pure PVA slime phantom (Figs. 3(a) and 4(a)). T1 value for water is approximately 4000 ms at 1.5T [16]. A higher T1 value obtained for distilled water from this study (5051 ms) was due to a higher precession of the spins in water surrounding at higher field (3 T) making it more difficult for energy to be transferred from the spins to the lattice as compared to a lower field (1.5 T) in which the precession is slower and the energy transfer is more efficient. The surrounding water molecules is said to have created a homogenous magnetic environment for the spins. For the pure PVA slime phantom, the T1 measured was 3948 ms, which is shorter than that of distilled water. The spins in the PVA slime phantom can be considered as being in a restricted (bound) state and the precession is slowed down much closer to the Larmor frequency, hence an easier energy transfer took place. In addition, the magnetic field is less homogenous in the surrounding molecules thus enabling more spin-lattice interaction. As longer T1 relaxation time means that the oscillation frequency of the spins in the surrounding molecules is much slower or faster than the Larmor frequency of the spins, there exist two extreme cases which are the ice at one end and free water at the other end. Thus, the distilled water and the PVA slime phantoms fabricated in this study should lie between these two extremes.

The addition of Gd_2O_3 into the matrix of the PVA slime phantom seemed to change the local magnetic field inhomogeneity of the surrounding as indicated by the reduction in the SNR_o value and the decrease in the T1 relaxation time. The local magnetic field inhomogeneity was suspected to increase with Gd_2O_3 addition which causes the

precession of the spins in the lattice occurs with a frequency that is near to the Larmor frequency of the spins, hence a shorter T1 relaxation process and T1 values as depicted in Table 4(a).

The exponential decrease in SNR value as a function of TE of distilled water and PVA slime phantom is related to the gradual decrease of transversal magnetization with time. Similar pattern is also observed for all Gd_2O_3-added phantoms. This typical T2 relaxation phenomenon resembles spin-spin interactions which gave rise to the decay of the magnetization in the *x*-*y* plane. In Figure 3(b) and 4(b), as TE increases, more signals are lost due to the decay process of transversal magnetization. Transversal magnetization is an unstable condition where it decays quickly after the termination of RF pulse. Distilled water and PVA slime phantoms show similar trend of decrease in SNR with increasing TE. The T2 relaxation time for distilled water and PVA slime phantoms were 246 ms and 197 ms respectively while the T2 relaxation time in Gd_2O_3-added phantoms decreases systematically with Gd_2O_3 concentration in the range of 197 ms to 97 ms (Table 4(b)). These values indicate that the change in T2 values is not as large as the change in T1 values with increasing Gd_2O_3 concentration. Thus, the relaxation modifier used in this study has a relatively small influence on T2 relaxation process. T2 relaxation process can also be explained on the basis of dipole-dipole interaction, predominantly the interaction between spins. The precession of a spin depends on the magnetic field, according to the Larmor equation [16]. When multiple spins are presence in a tissue, each spin's magnetic field will be superimposed on to the main magnetic field, which in turn affected the precession frequency of the others spins in the neighbourhood. For distilled water phantom, the molecules are quite mobile. For molecule that has properties similar to free water such as distilled water in this case, the difference in the precession frequencies between spins is small because the homogeneity of the magnetic field in which they are in is relatively high. The average effect is that the spins stay in precession state (minimal relaxation) longer resulting in a longer T2 (Figure 3(b)). For the pure PVA slime phantom, with the change in the molecular structure, magnetic field inhomogeneity increases, thus decreasing the duration in which the spins stay in phase. For Gd_2O_3-added phantoms, magnetic field inhomogeneity increases a bit more, reducing the T2 with further increase in Gd_2O_3 concentration (Figure 4(b)).

The relaxation rates for T1 and T2, (r_1 and r_2 respectively), shown in Figure 6 are usually used to measure the enhanced efficiency of the contrast agent [17]. From the observation made on T1 and T2 values for all the PVA slime phantoms, the plots of r_1 and r_2 vs. Gd_2O_3 concentration should show a positive linear relationship [17, 18], elucidating the increase in the rate of relaxation with increasing relaxation modifier concentration in the phantoms. Due to its slow respond in relaxation process, r_2 is always larger than r_1 at any Gd_2O_3 concentration. As discussed above, the presence of paramagnetic ions slowed down the precession of the spins by creating magnetic field inhomogeneity in the environment [19]. With the increase in Gd_2O_3 concentration in the PVA slime phantom, more Gd ions are present to interact with the spins thus increasing r_1 and r_2. To summarize, qualitatively the Gd_2O_3 added PVA slime phantom has several

potentials to be developed as MRI phantom. An extensive review about the quantitative treatment on MRI phantom can be found elsewhere [20].

CONCLUSION

In conclusion, the PVA slime phantoms fabricated in this study do have several potentials to be used as an alternative to the standard MRI water phantom as it demonstrates T1 and T2 characteristics that are similar to human tissues. When compared with distilled water phantom, pure PVA slime phantom has T1 and T2 relaxation times differ to that of the distilled water. By means of curve fitting method, all the phantoms displayed exponential behaviour from which the SNR value increases exponentially with TR (T1 curve) and decreases exponentially with TE (T2 curve). Furthermore, by adding the relaxation modifier (Gd_2O_3), the T1 and T2 characteristics of the PVA slime phantoms can be modified. With the systematic increase in Gd_2O_3 concentration, the SNR value decreases accordingly which further shortens the T1 and T2 relaxation times in a systematic manner. With this, a range of different T1 and T2 values can be obtained. The signal intensity of all the PVA slime phantoms with different Gd_2O_3 concentration is comparable. However, the results of this research are not conclusive as the number of phantoms that contained different Gd_2O_3 concentrations is limited. No information is gained on the reproducibility of the results and the stability of the phantoms. Therefore, a further research on a wider range of Gd_2O_3 concentrations as well as on the phantoms' stability and homogeneity over a long period of time are necessary.

ACKNOWLEDGMENT

The authors would like to thank Mr Sollahuddin Omar for his assistance in the preparation of PVA slime phantom. The authors would like to express gratitude to the Biomedical Sciences Program for the permission to use the equipment in the preparation of PVA slime phantom as well as the Department of Radiology, Hospital Canselor Tuanku Muhriz for the permission to use the MRI system. This research study was conducted under the research grant code of NN-2019-056.

REFERENCES

[1] T. M. Ihalainen, N. T. Lönnroth, J. I. Peltonen, J. K. Uusi-Simola, M. H. Timonen, L. J. Kuusela, S. E. Savolainen and O. E. Sipilä, *Acta Oncologica* **50(6)** 966–972 (2012).

[2] L. Friedman and H. H. Glover, *Journal of Magnetic Resonance Imaging* **23(6)** 827-839 (2006).

[3] K. Hattori, Y. Ikemoto, W. Takao, S. Ohno, T. Harimoto, S. Kanazawa, M. Oita, K. Shibuya, M. Kuroda and H. Kato, *Medical Physics* **40(3)** 032303 (2013).

[4] S. Ohno, H. Kato, T. Harimoto, Y. Ikemoto, K. Yoshitomi, S. Kadohisa, M. Kuroda and S. Kanazawa, *Magnetic Resonance in Medical Sciences* **7(3)** 131–

140 (2008).
[5] H. Kato, M. Kuroda, K. Yoshimura, A. Yoshida, K. Hanamoto, S. Kawasaki, K. Shibuya and S. Kanazawa *Medical Physics* **32(10)** 3199–3208 (2005).
[6] A. Hellerbach, V. Schuster, A. Jansen and J. Sommer *PLoS ONE* **8(8)** e70343 (2013).
[7] A. N. Yusoff, N. S. Abdul Rashid and S. Usman Ali *Journal of Physics Conference Series* **1083** 012017 (2018).
[8] Y. Ikemoto, W. Takao, K. Yoshitomi, S. Ohno, T. Harimoto, S. Kanazawa, K. Shibuya, M. Kuroda and H. Kato *Medical Physics* **38(11)** 6336 – 6342 (2011).
[9] M. D. Mitchell, H. L. Lundel, L. Axel and P. M. Joseph *Magnetic Resonance Imaging* **4(3)** 263–266 (1986).
[10] K. Yoshimura, H. Kato, M. Kuroda, A. Yoshida, K. Hanamoto, A. Tanaka, M. Tsunoda, S. Kanazawa, K. Shibuya, S. Kawasaki, Y. Hiraki *Magnetic Resonance in Medicine* **50(5)** 1011–1017 (2003).
[11] Y. Uchino, S. Shimmura, H. Miyashita, T. Taguchi, H. Kobayashi, J. Shimazaki, J. Tanaka and K. Tsubota. *Journal of Biomedical Materials Research Part B - Applied Biomaterials* **81(1)** 201–206. (2007).
[12] I. Mano, H. Goshima, M. Nambu and M. Iio *Magnetic Resonance in Medicine* **3(6)** 921–926 (1986).
[13] K. C. Chu and B. K. Rutt *Magnetic Resonance in Medicine* **37(2)** 314–319 (1997).
[14] E. Z. Casassa, A. M. Sarquis and C. H. Van Dyke. *Journal of Chemical Education* **63(1)** 57–60 (1986).
[15] O. Dietrich, J. G. Raya, S. Reeder, M. F. Reiser and S. O. Schoenberg *Journal of Magnetic Resonance Imaging* **26(2)** 375–385 (2007).
[16] A. D. Elster and J. H. Burdette *Questions and Answers in Magnetic Resonance Imaging* (2nd Ed.), Elsvier, Health Science Division: St. Louis, United States (2001).
[17] M. Engström, A. Klasson, H. Pedersen, C. Vahlberg, P. O. Käll and K. Uvdal *Magnetic Resonance Materials in Physics, Biology and Medicine* **19(4)**, 180–186, (2006).
[18] L. M. De Leõn-Rodríguez, A. F. Martins, M. C. Pinho, N. M. Rofsky and A. D. Sherry *Journal of Magnetic Resonance Imaging* 42(3), 545–565, (2015).
[19] K. A. Kraft, P. P. Fatouros, G. D. Clarke and P. R. S. Kishore *Magnetic Resonance in Medicine* **5(6),** 555–562, (1987).
[20] K. E. Keenan, M. Ainslie, A. J. Barker, M. A. Boss, K. M. Cecil, C. Charles, T. L. Chenevert, L. Clarke, J. L. Evelhoch, P. Finn, D. Gembris, J. L. Gunter, D. L. G. Hill, C. R. Jack Jr, E. F. Jackson, G. Liu, S. E. Russek, S. D. Sharma, M. Steckner, K. F. Stupic, J. D. Trzasko, C. Yuan, J. Zheng *Magnetic Resonance in Medicine* **79**, 48 – 61 (2018).